[5] Ketchum, E., and Tolson, R.,
Onboard star identification without a priori attitude information.
Journal of Guidance, Control and Dynamics, **18**, 2 (1995).

[6] Liebe C. C.
Accurancy performance of star trackers—A tutorial.
IEEE Transactions on Aerospace and Electronic Systems, **38**, 2 (Apr. 2002), 587–599.

[7] Mortari, D.
Search less algorithm for star pattern recognition.
The Journal of the Astronautical Sciences, **45**, 2 (Apr.–June 1997), 179–194.

[8] Mortari, D., and Angelucci, M.
Star pattern recognition and mirror assembly missalignment for Digistar II and III multiple FOVs star sensors.
Presented at the 9th Annual AIAA/AAS Space Flight Mechanics Meeting, Breckenridge, CO, Feb. 7–10, 1999, Paper AAS 99-192.

[9] Mortari, D., and Romoli, A.
StarNav III: A three fields of view star tracker.
IEEE Automatic Control paper 50, 2002, 47–57 (1).

[10] Padgett, C., and Kreutz-Delgado, K.
A grid algorithm for autonomous star identification.
IEEE Transactions on Aerospace and Electronic Systems, **33**, 1 (Jan. 1997), 202–213.

Detection of a Signal in Linear Subspace with Bounded Mismatch

We consider the problem of detecting a signal of interest in a background of noise with unknown covariance matrix, taking into account a possible mismatch between the actual steering vector and the presumed one. We assume that the former belongs to a known linear subspace, up to a fraction of its energy. When the subspace of interest consists of the presumed steering vector, this amounts to assuming that the angle between the actual steering vector and the presumed steering vector is upper bounded. Within this framework, we derive the generalized likelihood ratio test (GLRT). We show that it involves solving a minimization problem with the constraint that the signal of interest lies inside a cone. We present a computationally efficient algorithm to find the maximum likelihood estimator (MLE) based on the Lagrange multiplier technique. Numerical simulations illustrate the performance and the robustness of this new detector, and compare it with the adaptive coherence estimator which assumes that the steering vector lies entirely in a subspace.

Manuscript received August 30, 2005; revised January 24, 2006; released for publication March 15, 2006.

IEEE Log No. T-AES/42/3/878254.

Refereeing of this contribution was handled by E. S. Chornoboy.

I. INTRODUCTION

Detecting a signal of interest in a background of noise is a fundamental task in many array processing applications, notably in radar systems whose core task is to detect a target against clutter and thermal noise (and possibly jamming). Usually, the presence of a target with given space or space-time signature is sought in a vector under test, using secondary data which consists of noise only. This problem has been extensively studied and a large number of solutions have appeared in the literature, that depend on the assumptions made on the statistical properties of the noise, see e.g. [1] for a very good list of references. Under the Gaussian assumption, the most celebrated detectors are Kelly's generalized likelihood ratio test (GLRT) [2] and the adaptive matched filter (AMF) of Robey et al. [3]. Both detectors assume a homogeneous environment, i.e., the noise covariance matrix of the primary vector is identical to the noise covariance matrix of the secondary data. Kelly's detector is based on the GLRT principle using the whole data, viz. the primary and secondary data. In contrast, the AMF first proceeds with the primary data, assuming that the noise covariance matrix is known. Then, the latter is substituted for its maximum likelihood estimate (MLE) using the secondary data. The performances of these two detectors have been evaluated thoroughly on simulated data in [2] and [3] as well as on real data, see e.g. [4, 5]. In the partially homogeneous case, i.e., when the noise covariance matrices in the primary and secondary data have the same structure but possibly different levels, a benchmark detector is the adaptive coherence estimator (ACE). The ACE was originally proposed in [6] and [7] as an adaptive version of the constant false-alarm rate (CFAR) matched subspace detectors of [8]. It was also independently developed in [9] and [10] in the case of compound-Gaussian noise. It turns out that, under the Gaussian assumption, the ACE is the GLRT for the problem at hand [11]. Furthermore, it was shown to be the uniformly most powerful invariant (UMPI) test [12–14].

All detectors above, and in general most detectors, assume a precise knowledge of the space or space-time signature of interest (we'll refer to it as the steering vector in the sequel). However, in practice, there potentially exist many reasons for this assumption not to hold. These include uncalibrated arrays, pointing errors, spatially dispersed targets, wavefront distorsions, etc. When the presumed steering vector, that is the steering vector whose presence is to be detected, differs from the actual steering vector, detection performance loss is incurred [3, 15, 16].[1] Quoting from [15] this loss may be

[1] Performance analysis of some detection schemes under general types of mismatch (notably covariance mismatches between the test vector and the training samples) can be found in [17]–[20].

more significant than expected from the sidelobes levels of the adapted pattern. Therefore, it is of interest to take into account the possible steering vector mismatch at the design stage of the detector. This approach is relatively scarce in the literature, at least for detection problems. In contrast, it has received considerable attention recently in the field of adaptive beamforming, see e.g. [21–24], where worst case approaches are advocated to make the Capon beamformer more robust to steering vector errors. Obviously, taking into account steering vector uncertainties requires modeling of the latter. A possible approach is to assume that the steering vector belongs to a known linear subspace. This is essentially what the multi-rank ACE of [6] does, see also [25] for an extension to multiple observations in the primary data. The interest of this modeling is that it leads to closed-form and rather simple detectors, which additionally possess the CFAR property. The only drawback concerns the choice of the subspace as one should ensure that the actual steering vector belongs to it, which is not obvious a priori. Of course, the size of the subspace can be increased, but at the detriment of detection performance. Another option is proposed in [26] where the actual steering vector is assumed to belong to a cone whose axis is the presumed steering vector. One-step and two-step GLRTs are derived in [26]. Unfortunately, maximum likelihood estimation of the steering vector leads to an optimization problem which is not convex. In order to remedy this pitfall, the problem is reformulated as four optimization problems, each of them being convex. Then, second-order cone programming techniques are used to compute the solution. However, the overall complexity of the detector is relatively high. In this work, we combine the two ideas above by assuming that the steering vector belongs to a linear subspace with bounded mismatch. In other words, most of its energy is inside a subspace but a fraction of it can lie outside the subspace. This modeling allows more flexibility than the pure subspace approach and also eases the choice of the subspace, as we allow the steering vector not to be strictly in a subspace. The model used here belongs to the general framework of cone classes [27] and is thus related to [26]. However, it will be shown that the MLE of the steering vector can be obtained using the technique of Lagrange multipliers, which results in a less complicated detector. Furthermore, the case of a partially homogeneous environment is considered here, i.e., the covariance matrix of the primary and secondary data have the same structure but a possibly different level. This is to be contrasted with [26] where a homogeneous environment is considered.

II. GENERALIZED LIKELIHOOD RATIO TEST

We assume that data are collected from m sensors and denote $\mathbf{z}$ the m-length vector under test. We also assume that K training samples $\mathbf{z}_k$, which contain noise only, are available. The detection problem considered here is that of deciding between the following two hypotheses

$$\begin{aligned} H_0:&\ \begin{cases} \mathbf{z}=\mathbf{n} \\ \mathbf{z}_k=\mathbf{n}_k; \qquad k=1,\ldots,K \end{cases} \\ H_1:&\ \begin{cases} \mathbf{z}=\mathbf{s}+\mathbf{n} \\ \mathbf{z}_k=\mathbf{n}_k; \qquad k=1,\ldots,K. \end{cases} \end{aligned} \tag{1}$$

In (1), $\mathbf{n}$ and $\mathbf{n}_k$ are proper zero-mean independent and Gaussian distributed noise vectors with covariance matrices

$$\mathcal{E}\{\mathbf{n}\mathbf{n}^H\}=\gamma\mathbf{M} \tag{2a}$$

$$\mathcal{E}\{\mathbf{n}_k\mathbf{n}_k^H\}=\mathbf{M}. \tag{2b}$$

Hence, we consider a partially homogeneous environment in which the covariance matrices of the primary and the secondary data have the same structure, but possibly different power. We assume that the steering vector of interest $\mathbf{s}$ belongs to a linear subspace, spanned by the columns of the $m\times p$ matrix $\bar{\mathbf{A}}$, with a bounded mismatch. In other words, the fraction of energy of $\mathbf{s}$ outside $\mathcal{R}(\bar{\mathbf{A}})$ is bounded, which can be formulated mathematically as

$$\mathbf{s}\in\mathcal{C}=\left\{\mathbf{s};\frac{\mathbf{s}^H\mathbf{P}_{\bar{\mathbf{A}}}\mathbf{s}}{\mathbf{s}^H\mathbf{s}}\geq\rho\right\} \tag{3}$$

where $\mathbf{P}_{\bar{\mathbf{A}}}$ is the orthogonal projection onto $\mathcal{R}(\bar{\mathbf{A}})$, and $0<\rho<1$ is a scalar that sets how much of the energy is allowed to be outside $\mathcal{R}(\bar{\mathbf{A}})$. In the limiting case $\rho=1$, $\mathbf{s}\in\mathcal{R}(\bar{\mathbf{A}})$. Of special interest to us is the case $p=1$ where $\bar{\mathbf{A}}=\bar{\mathbf{a}}$ is the presumed steering vector. In this case, (3) can be rewritten as

$$\mathbf{s}\in\mathcal{C}=\left\{\mathbf{s};\frac{|\mathbf{s}^H\bar{\mathbf{a}}|^2}{(\mathbf{s}^H\mathbf{s})(\bar{\mathbf{a}}^H\bar{\mathbf{a}})}\geq\rho\right\}. \tag{4}$$

The constraint (4) means that the square of the cosine angle between $\mathbf{s}$ and $\bar{\mathbf{a}}$ must be above ρ. Again, when $\rho=1$, the actual steering vector is aligned with the presumed steering vector.

In the sequel, we derive the GLRT for the problem described in (1). Let $\mathbf{Z}=[\mathbf{z}_1,\ldots,\mathbf{z}_K]$ denote the secondary data matrix. Under the assumptions made, the joint probability density function (pdf) of $\mathbf{z}$ and $\mathbf{Z}$ is given by [8]

$$\begin{aligned} f(\mathbf{z},\mathbf{Z})&=\frac{\exp\{-\gamma^{-1}(\mathbf{z}-\mu\mathbf{s})^H\mathbf{M}^{-1}(\mathbf{z}-\mu\mathbf{s})\}}{\pi^m\gamma^m|\mathbf{M}|}\times\frac{\exp\{-\sum_{k=1}^K\mathbf{z}_k^H\mathbf{M}^{-1}\mathbf{z}_k\}}{\pi^{mK}|\mathbf{M}|^K} \\ &=\left\{\frac{e^{-\mathrm{Tr}\{\mathbf{M}^{-1}\mathbf{T}\}}}{\pi^m\gamma^{m/(K+1)}|\mathbf{M}|}\right\}^{K+1} \end{aligned} \tag{5}$$

with

$$\mathbf{T} = \frac{1}{K+1}\left\{\gamma^{-1}(\mathbf{z}-\mu\mathbf{s})(\mathbf{z}-\mu\mathbf{s})^H + \sum_{k=1}^{K}\mathbf{z}_k\mathbf{z}_k^H\right\}. \quad (6)$$

In the previous equations, Tr{.} and |.| stand for the trace and the determinant, respectively, and $\mu = 0$ under H_0, $\mu = 1$ under H_1. It is well known [2] that the MLE of $\mathbf{M}$ is $\hat{\mathbf{M}} = \mathbf{T}$. Substituting this value in (5), it follows that

$$\max_{\mathbf{M}} f(\mathbf{z},\mathbf{Z}) = \{(e\pi)^m|\mathbf{T}|\gamma^{m/(K+1)}\}^{-(K+1)}. \quad (7)$$

Let us note

$$\mathbf{S} = \sum_{k=1}^{K}\mathbf{z}_k\mathbf{z}_k^H \quad (8)$$

the sample covariance matrix of the secondary data. Using the fact that

$$|\mathbf{T}| = \frac{|\mathbf{S}|}{(K+1)^m}\{1+\gamma^{-1}(\mathbf{z}-\mu\mathbf{s})^H\mathbf{S}^{-1}(\mathbf{z}-\mu\mathbf{s})\} \quad (9)$$

it is straightforward to show that the maximum of the right-hand side of (7) with respect to γ is attained (see [11] for a similar derivation) when

$$\gamma = \gamma_0 = \frac{K+1-m}{m}(\mathbf{z}-\mu\mathbf{s})^H\mathbf{S}^{-1}(\mathbf{z}-\mu\mathbf{s}). \quad (10)$$

With this value of γ, $|\mathbf{T}|$ becomes a constant, and therefore

$$\max_{\gamma,\mathbf{M}} f(\mathbf{z},\mathbf{Z}) \propto \{(\mathbf{z}-\mu\mathbf{s})^H\mathbf{S}^{-1}(\mathbf{z}-\mu\mathbf{s})\}^{-m}. \quad (11)$$

Consequently, the generalized likelihood ratio (GLR) can be written as

$$\mathrm{GLR} = \left\{\frac{\mathbf{z}^H\mathbf{S}^{-1}\mathbf{z}}{\min_{\mathbf{s}\in\mathcal{C}}(\mathbf{z}-\mathbf{s})^H\mathbf{S}^{-1}(\mathbf{z}-\mathbf{s})}\right\}^m. \quad (12)$$

The last step to complete the derivation of the GLRT consists of solving the minimization problem at the denominator of (12). When $\mathbf{s}$ completely belongs to $\mathcal{R}(\bar{\mathbf{A}})$, this minimization problem admits a closed-form solution, namely

$$\begin{aligned}\hat{\mathbf{s}}_1 &= \arg\min_{\mathbf{s}\in\mathcal{R}(\bar{\mathbf{A}})}(\mathbf{z}-\mathbf{s})^H\mathbf{S}^{-1}(\mathbf{z}-\mathbf{s}) \\ &= \bar{\mathbf{A}}(\bar{\mathbf{A}}^H\mathbf{S}^{-1}\bar{\mathbf{A}})^{-1}\bar{\mathbf{A}}^H\mathbf{S}^{-1}\mathbf{z}. \end{aligned} \quad (13)$$

In contrast, when $\mathbf{s}\in\mathcal{C}$, a closed-form solution cannot generally be found. At least two cases should be considered. First, if $\mathbf{z}\in\mathcal{C}$ then $\mathbf{z}$ is necessarily the solution. In this case, the vector under test is close to the presumed steering vector. The denominator in (12) is zero and a detection is always declared. This is not an issue under H_1. In fact, in high signal to noise ratio, $\mathbf{z} = \mathbf{s} + \mathbf{n}$ may be close to $\mathbf{s}$, and thus can belong to the cone. In such a case the signal is detected, which is the desired result. In contrast, under the null hypothesis, the fact that $\mathbf{z}\in\mathcal{C}$ is a problem as it causes a false alarm. In Appendix A, we derive the probability that, under H_0, the vector under test $\mathbf{z}$ is inside the cone. It appears that this probability is very small, and indeed much smaller than the probabilities of false alarm usually considered. The probability that $\mathbf{z}\in\mathcal{C}$ under H_0 mostly depends on the cone angle θ_c. Therefore, attention should be paid not to choose a too large θ_c; at least, one must ensure that the probability of false alarm chosen is larger than $\Pr(\mathbf{z}\in\mathcal{C}\mid H_0)$. In any case, the latter is a lower bound on the the probability of false alarm. We now concentrate on the case where $\mathbf{z}\notin\mathcal{C}$. In such a situation, there is no closed-from solution to the minimization problem and we resort to the Lagrange multiplier technique to solve it [28]. The Lagrangian can be written as

$$L(\mathbf{s},\lambda) = (\mathbf{z}-\mathbf{s})^H\mathbf{S}^{-1}(\mathbf{z}-\mathbf{s}) + \lambda(\rho\mathbf{s}^H\mathbf{s} - \mathbf{s}^H\mathbf{P}_{\bar{\mathbf{A}}}\mathbf{s}) \quad (14)$$

where $\lambda\geq 0$ is the real-valued Lagrange multiplier. For the sake of notational convenience, let us define

$$\mathbf{Q} = \rho\mathbf{I} - \mathbf{P}_{\bar{\mathbf{A}}} \quad (15a)$$

$$\mathbf{W} = \mathbf{S}^{-1} + \lambda\mathbf{Q}. \quad (15b)$$

In the present case, with a single inequality constraint, if there is a strictly feasible point, i.e., a vector $\mathbf{s}$ such that $\rho\mathbf{s}^H\mathbf{s} - \mathbf{s}^H\mathbf{P}_{\bar{\mathbf{A}}}\mathbf{s} < 0$, there is a zero duality gap between the primal and the dual problem [28]. In our case, there exists a vector that is strictly feasible, for instance any vector in $\mathcal{R}(\bar{\mathbf{A}})$. This means that the optimal value of the initial minimization problem in (12) will be the same as the optimal value of the dual problem. Therefore, we consider the dual problem. Completing the squares, we can rewrite (14) as

$$\begin{aligned}L(\mathbf{s},\lambda) &= [\mathbf{s}-\mathbf{W}^{-1}\mathbf{S}^{-1}\mathbf{z}]^H\mathbf{W}[\mathbf{s}-\mathbf{W}^{-1}\mathbf{S}^{-1}\mathbf{z}] \\ &\quad + \mathbf{z}^H\mathbf{S}^{-1}\mathbf{z} - \mathbf{z}^H\mathbf{S}^{-1}\mathbf{W}^{-1}\mathbf{S}^{-1}\mathbf{z}. \end{aligned} \quad (16)$$

Hence, the dual function is [28]

$$\begin{aligned}g(\lambda) &= \min_{\mathbf{s}} L(\mathbf{s},\lambda) \\ &= \mathbf{z}^H\mathbf{S}^{-1}\mathbf{z} - \mathbf{z}^H\mathbf{S}^{-1}\mathbf{W}^{-1}\mathbf{S}^{-1}\mathbf{z} \end{aligned} \quad (17)$$

provided that $\mathbf{W} = \mathbf{S}^{-1} + \lambda\mathbf{Q} > 0$. Otherwise, the dual function is unbounded below and takes the value $-\infty$. The vector $\mathbf{s}$ which minimizes $L(\mathbf{s},\lambda)$ is given by

$$\hat{\mathbf{s}}(\lambda) = \mathbf{W}^{-1}\mathbf{S}^{-1}\mathbf{z} \quad (18)$$

where we emphasize that λ is still to be determined. In order to obtain the latter, we need to maximize the dual function [28], which amounts to minimizing

$$f(\lambda) = \mathbf{z}^H\mathbf{S}^{-1}\mathbf{W}^{-1}\mathbf{S}^{-1}\mathbf{z} \quad (19)$$

with respect to $\lambda\geq 0$. Let λ_0 be the minimizer of $f(\lambda)$ and $\hat{\mathbf{s}}_0 = \hat{\mathbf{s}}(\lambda_0)$. Setting the derivative of $f(\lambda)$ to zero

yields

$$f'(\lambda) = \mathbf{z}^H \mathbf{S}^{-1} \frac{\partial \mathbf{W}^{-1}}{\partial \lambda} \mathbf{S}^{-1} \mathbf{z} = -\mathbf{z}^H \mathbf{S}^{-1} \mathbf{W}^{-1} \mathbf{Q} \mathbf{W}^{-1} \mathbf{S}^{-1} \mathbf{z} = 0. \quad (20)$$

Observing that $f'(\lambda) = \hat{\mathbf{s}}^H(\lambda)\mathbf{Q}\hat{\mathbf{s}}(\lambda)$, it follows that minimization of $f(\lambda)$ will yield a vector $\hat{\mathbf{s}}_0$ which lies on the boundary of the cone, and hence $\hat{\mathbf{s}}_0$ is the sought solution; see also Remark 1 below. In order to minimize $f(\lambda)$, we rewrite it in a more convenient form. Let

$$\mathbf{S}^{1/2}\mathbf{Q}\mathbf{S}^{1/2} = \mathbf{U}\boldsymbol{\Gamma}\mathbf{U}^H \quad (21)$$

be the eigenvalue decomposition of $\mathbf{S}^{1/2}\mathbf{Q}\mathbf{S}^{1/2}$ with $\mathbf{S}^{1/2}$ a square root of $\mathbf{S}$, and where the eigenvalues are arranged in decreasing order. Then we have

$$\begin{aligned} f(\lambda) &= \mathbf{z}^H \mathbf{S}^{-1} [\mathbf{S}^{-1} + \lambda \mathbf{Q}]^{-1} \mathbf{S}^{-1} \mathbf{z} \\ &= \mathbf{z}^H \mathbf{S}^{-1/2} [\mathbf{I} + \lambda \mathbf{S}^{1/2} \mathbf{Q} \mathbf{S}^{1/2}]^{-1} \mathbf{S}^{-1/2} \mathbf{z} \\ &= \mathbf{z}^H \mathbf{S}^{-1/2} \mathbf{U} [\mathbf{I} + \lambda \boldsymbol{\Gamma}]^{-1} \mathbf{U}^H \mathbf{S}^{-1/2} \mathbf{z} \\ &= \mathbf{x}^H [\mathbf{I} + \lambda \boldsymbol{\Gamma}]^{-1} \mathbf{x} \\ &= \sum_{k=1}^{m} \frac{|x_k|^2}{1 + \lambda \gamma_k}. \end{aligned} \quad (22)$$

We now show how to minimize $f(\lambda)$. First, note that $\mathbf{Q}$ has $m - p$ positive eigenvalues equal to ρ and p negative eigenvalues equal to $\rho - 1$. Since $\mathbf{Q}$ and $\mathbf{S}^{1/2}\mathbf{Q}\mathbf{S}^{1/2}$ have the same inertia [29], we have $\gamma_1 > \cdots > \gamma_{m-p} > 0 > \gamma_{m-p+1} > \cdots > \gamma_m$. Moreover, since $\mathbf{S}^{-1} + \lambda\mathbf{Q} = \mathbf{S}^{-1/2}(\mathbf{I} + \lambda\mathbf{S}^{1/2}\mathbf{Q}\mathbf{S}^{1/2})\mathbf{S}^{-1/2}$ must be positive, we must have $1 + \lambda\gamma_k > 0$, $\forall k$, and hence $0 \le \lambda < -1/\gamma_m$. Therefore, $f(\lambda)$ should be minimized in the interval $[0, -\gamma_m^{-1}]$. We now show that, in this interval, there exists a unique value of λ for which $f'(\lambda) = 0$. Observe that

$$f''(\lambda) = 2\sum_{k=1}^{m} \frac{\gamma_k^2 |x_k|^2}{(1 + \lambda\gamma_k)^3} \quad (23)$$

is positive in $[0, -\gamma_m^{-1}]$, and therefore $f'(\lambda)$ is monotonically increasing in this interval. Moreover, for $\lambda = 0$, $\mathbf{W} = \mathbf{S}^{-1}$ and then, according to (20)

$$f'(0) = -\mathbf{z}^H \mathbf{Q} \mathbf{z} < 0 \quad (24)$$

as $\mathbf{z} \notin \mathcal{C}$. Additionally,

$$\lim_{\lambda \to (-\gamma_m^{-1})^-} f'(\lambda) = +\infty. \quad (25)$$

Hence, there exists a unique value $\lambda_0 \in [0, -\gamma_m^{-1}]$ for which $f'(\lambda_0) = 0$. This unique value provides the solution $\hat{\mathbf{s}}_0 = \hat{\mathbf{s}}(\lambda_0)$ of the minimization problem of (12). Additionally, since $f'(\lambda)$ is monotonically increasing and has a unique zero, computationally efficient techniques such as the Newton method can be used to find λ_0.

REMARK 1 An alternative but similar route can be taken to obtain the MLE of $\mathbf{s}$. First, note that, at the solution, the inequality constraint is active, i.e., the solution lies on the boundary of the cone. To see this, assume that the solution $\mathbf{s}_0$ is strictly inside the cone, i.e., $\mathbf{s}_0^H \mathbf{Q} \mathbf{s}_0 < 0$. Then, consider $\mathbf{s}_1 = \mathbf{s}_0 + \mu(\mathbf{z} - \mathbf{s}_0)$ with $0 \le \mu \le 1$. Obviously

$$\begin{aligned} (\mathbf{z} - \mathbf{s}_1)^H \mathbf{S}^{-1} (\mathbf{z} - \mathbf{s}_1) &= (1 - \mu)^2 (\mathbf{z} - \mathbf{s}_0)^H \mathbf{S}^{-1} (\mathbf{z} - \mathbf{s}_0) \\ &\le (\mathbf{z} - \mathbf{s}_0)^H \mathbf{S}^{-1} (\mathbf{z} - \mathbf{s}_0). \end{aligned}$$

Furthermore, we can always find a $\mu \in [0, 1]$ such that $\mathbf{s}_1^H \mathbf{Q} \mathbf{s}_1 = 0$. Indeed,

$$h(\mu) = \mathbf{s}_1^H \mathbf{Q} \mathbf{s}_1 = [\mathbf{s}_0 + \mu(\mathbf{z} - \mathbf{s}_0)]^H \mathbf{Q} [\mathbf{s}_0 + \mu(\mathbf{z} - \mathbf{s}_0)]$$

is a continuous function of μ. Additionally, $h(0) = \mathbf{s}_0^H \mathbf{Q} \mathbf{s}_0 < 0$ and $h(1) = \mathbf{z}^H \mathbf{Q} \mathbf{z} > 0$. Therefore, there exists a μ such that $h(\mu) = 0$. This is in contradiction with the fact that $\mathbf{s}_0$ is the solution. Hence, the inequality constraint may be replaced by an equality constraint. The Lagrangian is still given by (14). Solving for the stationary point of $L(\mathbf{s}, \lambda)$ yields the solution $\hat{\mathbf{s}}(\lambda) = \mathbf{W}^{-1}\mathbf{S}^{-1}\mathbf{z}$ of (18). Next, λ is obtained by enforcing the equality constraint, i.e., $\hat{\mathbf{s}}^H(\lambda)\mathbf{Q}\hat{\mathbf{s}}(\lambda) = 0$, which leads to (20). Then, λ is obtained via the procedure described above.

The minimization problem is pictorially depicted in Fig. 1 in the simple case $m = 2$ (and with real-valued $\mathbf{s}$, $\mathbf{z}$, etc.…). The contours of $(\mathbf{z} - \mathbf{s})^H \mathbf{S}^{-1} (\mathbf{z} - \mathbf{s})$ are ellipses centered at $\mathbf{z}$ while the boundaries of $\mathcal{C}$ are lines. The size of the ellipse is increased (via λ) until the gradient of the ellipse becomes orthogonal to the border line of the cone [30]. We also display the trajectory of $\hat{\mathbf{s}}(\lambda)$ as λ goes from 0—in which case $\hat{\mathbf{s}}(0) = \mathbf{z}$—and is progressively increased. The solution is found when λ is such that the ellipse becomes tangent to the border line of the cone. Note that the solution $\hat{\mathbf{s}}_0$ satisfies $(\mathbf{z} - \hat{\mathbf{s}}_0)^H \mathbf{S}^{-1} \hat{\mathbf{s}}_0 = 0$ [27]; in other words, $\mathbf{S}^{-1/2}\hat{\mathbf{s}}_0$ is the projection of $\mathbf{S}^{-1/2}\mathbf{z}$ onto the surface of the (whitened) cone.

Once the MLE of $\mathbf{s}$ is obtained, it can be substituted in (12) to yield the GLRT. Using the fact that

$$(\mathbf{z} - \hat{\mathbf{s}}_0)^H \mathbf{S}^{-1} (\mathbf{z} - \hat{\mathbf{s}}_0) = \mathbf{z}^H \mathbf{S}^{-1} \mathbf{z} - \mathbf{z}^H \mathbf{S}^{-1} \hat{\mathbf{s}}_0$$

it ensues that the GLRT can be rewritten in the following equivalent form

$$\frac{\mathbf{z}^H \mathbf{S}^{-1} \hat{\mathbf{s}}_0}{\mathbf{z}^H \mathbf{S}^{-1} \mathbf{z}} \underset{H_0}{\overset{H_1}{\gtrless}} \eta_{\text{GLRT}}. \quad (26)$$

A few observations are in order regarding the invariances of the problem considered here, and those of the corresponding problem when $\mathbf{s}$ is known to belong to $\mathcal{R}(\bar{\mathbf{A}})$. For the sake of simplicity, consider

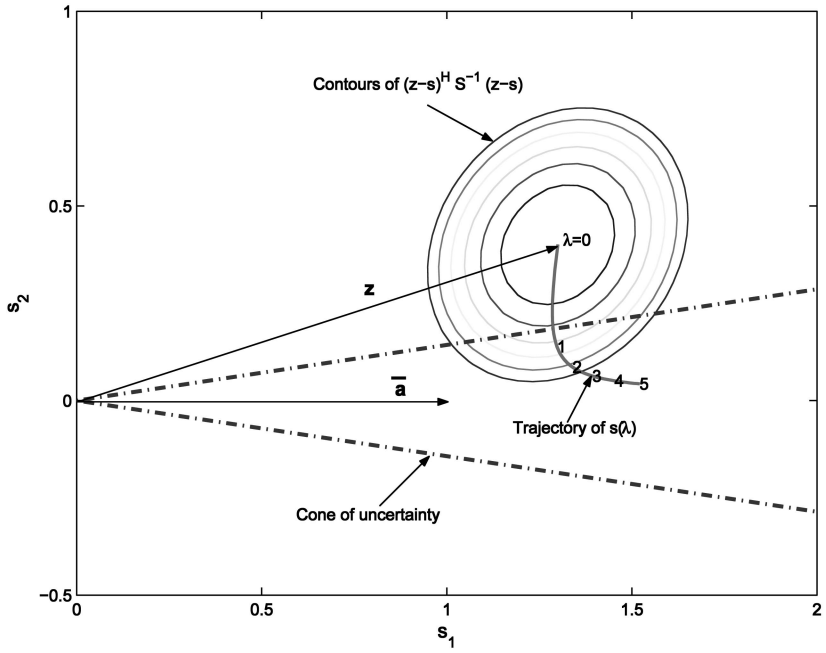

Fig. 1. Geometry of minimization problem $\min_{\mathbf{s}\in\mathcal{C}}(\mathbf{z}-\mathbf{s})^H\mathbf{S}^{-1}(\mathbf{z}-\mathbf{s})$ when $m=2$.

the case $p=1$. Then, see [11], the ACE is the GLRT for the detection problem

$$\begin{aligned} H_0:&\quad \begin{cases} \mathbf{z}=\mathbf{n} \\ \mathbf{z}_k=\mathbf{n}_k; & k=1,\ldots,K \end{cases} \\ H_1:&\quad \begin{cases} \mathbf{z}=\mathbf{s}+\mathbf{n}; & \mathbf{s}\propto\bar{\mathbf{a}} \\ \mathbf{z}_k=\mathbf{n}_k; & k=1,\ldots,K. \end{cases} \end{aligned} \tag{27}$$

The detection problem (27) is invariant under the group of transformations [12, 14]

$$G=\{g:\ [\mathbf{z}\ \ \mathbf{Z}]\rightarrow[\beta\mathbf{T}\mathbf{z}\ \ \mathbf{T}\mathbf{Z}\mathbf{V}^H]\} \tag{28}$$

where β is an arbitrary scalar, $\mathbf{V}$ is an $K\times K$ unitary matrix, and $\mathbf{T}$ is an $m\times m$ full-rank matrix such that

$$\mathbf{T}\bar{\mathbf{a}}\propto\bar{\mathbf{a}}. \tag{29}$$

The specific form of this group can be briefly explained as follows. Since all data vectors are Gaussian distributed, attention should be restricted to linear transformations. The unitary matrix $\mathbf{V}$ preserves independence of the columns of $\mathbf{Z}$. The presence of the arbitrary scalar β is due to the fact that one does not know the scaling factor between the covariance matrix of $\mathbf{z}$ and that of the columns of $\mathbf{Z}$. Finally, the matrix $\mathbf{T}$ should be full rank, in order for the transformed covariance matrix to be full rank. Moreover, the mean of $\mathbf{z}$ under H_1 should be proportional to $\bar{\mathbf{a}}$, which explains why $\mathbf{T}\bar{\mathbf{a}}\propto\bar{\mathbf{a}}$. The ACE is invariant to this group of transformations. Moreover, for the detection problem stated in (27), the ACE is the uniformly most powerful test within all tests that are invariant to G [14].

In contrast, the detector in (26) is not invariant to G, at least when $\mathbf{T}\bar{\mathbf{a}}\propto\bar{\mathbf{a}}$. On the other hand, the transformations in (28)–(29) are not the invariances for the problem at hand, and it is not expressly required that a detector for the problem in (1) be invariant to them. This rises the question of the invariances of (1). Given the similarity between (1) and (27), the group of transformations under which (1) is invariant is still given by (28), except that the matrix $\mathbf{T}$ is now required to leave the cone invariant, instead of only leaving $\bar{\mathbf{a}}$ invariant. However, the natural invariances of a cone are scaling, rotation around its axis and symmetry with respect to the hyperplane orthogonal to $\bar{\mathbf{a}}$. Therefore, the transformations $\mathbf{T}$ that leave the cone invariant are of the form [8]

$$\mathbf{T}=\alpha[\mathbf{P}_{\bar{\mathbf{a}}}+\mathbf{U}_{\bar{\mathbf{a}}}^{\perp}\mathbf{Q}\mathbf{U}_{\bar{\mathbf{a}}}^{\perp H}] \tag{30}$$

where α is an arbitrary scalar, $\mathbf{P}_{\bar{\mathbf{a}}}$ is the orthogonal projection onto $\bar{\mathbf{a}}$, $\mathbf{U}_{\bar{\mathbf{a}}}^{\perp}$ is an $m\times(m-1)$ matrix whose columns form an orthonormal basis for $\mathcal{R}(\bar{\mathbf{a}})^{\perp}$, and $\mathbf{Q}$ is a unitary matrix. The matrix $\mathbf{T}$ above (ignoring the scaling factor α) retains the component of $\mathbf{s}$ along $\bar{\mathbf{a}}$, while the orthogonal component is rotated around $\bar{\mathbf{a}}$. To summarize, the invariances of the present detection problem are described by (28) and (30). It is straightforward to show that the GLRT is indeed invariant to these transformations. Indeed, if $\mathbf{z}$ and $\mathbf{Z}$ are transformed as in (28) with $\mathbf{T}$ given by (30), then $\mathbf{S}\rightarrow|\beta|^2\mathbf{T}\mathbf{S}\mathbf{T}^H$, $\hat{\mathbf{s}}_0\rightarrow\beta\mathbf{T}\hat{\mathbf{s}}_0$ and thus the GLRT is invariant. However, the detector in (26) cannot be claimed to possess the CFAR property with respect to the noise covariance matrix. Finally, observe that even if it happens that $\mathbf{s}\propto\bar{\mathbf{a}}$, the ACE is not necessarily optimal for the detection problem considered herein, unless the invariance to the transformations in (28)–(29) is enforced.

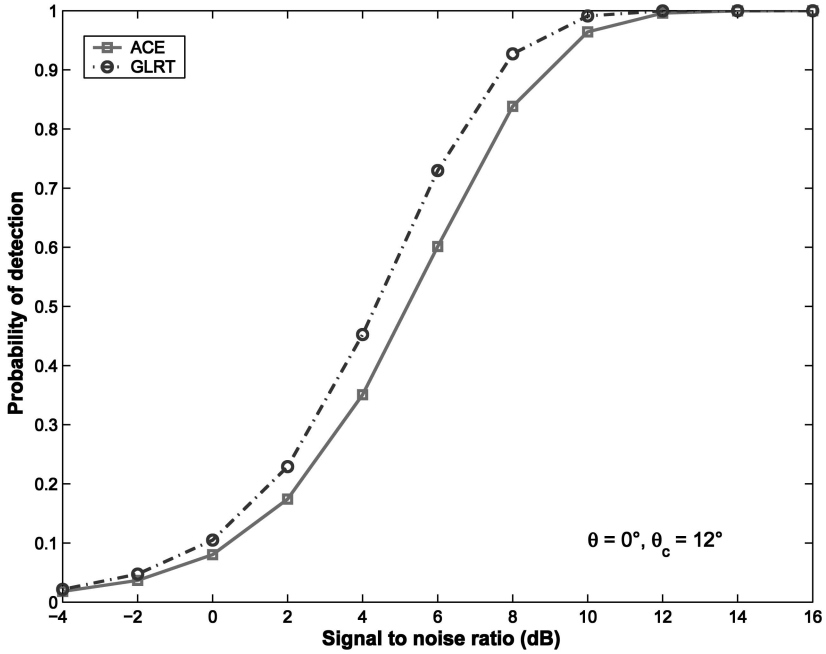

Fig. 2. Probability of detection versus SNR. $\theta = 0^\circ$ and $\theta_c = 12^\circ$.

As a final remark, notice that the ACE is given by

$$\frac{\mathbf{z}^H\mathbf{S}^{-1}\hat{\mathbf{s}}_1}{\mathbf{z}^H\mathbf{S}^{-1}\mathbf{z}} \underset{H_0}{\overset{H_1}{\gtrless}} \eta_{\text{ACE}}. \tag{31}$$

However, since $\hat{\mathbf{s}}_1 \in \mathcal{C}$,

$$(\mathbf{z}-\hat{\mathbf{s}}_0)^H\mathbf{S}^{-1}(\mathbf{z}-\hat{\mathbf{s}}_0) \le (\mathbf{z}-\hat{\mathbf{s}}_1)^H\mathbf{S}^{-1}(\mathbf{z}-\hat{\mathbf{s}}_1) \tag{32}$$

which implies that

$$\frac{\mathbf{z}^H\mathbf{S}^{-1}\hat{\mathbf{s}}_0}{\mathbf{z}^H\mathbf{S}^{-1}\mathbf{z}} \ge \frac{\mathbf{z}^H\mathbf{S}^{-1}\hat{\mathbf{s}}_1}{\mathbf{z}^H\mathbf{S}^{-1}\mathbf{z}}. \tag{33}$$

The GLRT with a signal in the cone is thus lower bounded by the multi-rank ACE.

III. NUMERICAL ILLUSTRATIONS

In this section, we assess the performance of the GLRT as well as its robustness, and compare it with the ACE. We focus on the case $p = 1$ and let $\bar{\mathbf{a}}$ denote the presumed steering vector. We let θ denote the angle between $\mathbf{s}$ and $\bar{\mathbf{a}}$ while θ_c denotes the angle of the cone in which $\mathbf{s}$ is assumed to lie, i.e., $\cos^2\theta_c = \rho$. In order to test the performance and the robustness of the GLRT and the ACE, we consider two scenarios, namely $\theta = 0$, i.e., the actual signal of interest is aligned with $\bar{\mathbf{a}}$, and $\theta \neq 0$.

In all simulations, we consider an array with $m = 8$ elements and an exponentially-shaped noise covariance matrix, viz. the (k,ℓ)th element of $\mathbf{M}$ is

$$\mathbf{M}_{k,\ell} = \alpha^{|k-\ell|} \tag{34}$$

and $\alpha = 0.9$ in the simulations below. In order to set the thresholds η_{GLRT} and η_{ACE} for a given probability of false alarm P_{fa}, we resorted to Monte-Carlo counting techniques. More precisely, 10^6 simulations of the data under the null hypothesis were run, and the test statistics in (26) and (31) were computed and sorted. The thresholds were set from the $1 - P_{fa}$ quantile. In the simulations shown below, $P_{fa} = 10^{-3}$. Note that this P_{fa} is well above the probability that the test vector $\mathbf{z}$ belongs to the cone under H_0. Indeed, assuming white Gaussian noise, it is shown in Appendix A that $\Pr(\mathbf{z} \in \mathcal{C} \mid H_0) = 2.82\ 10^{-10}$ when the cone angle is $\theta_c = 12^\circ$, as is the case in the simulations presented below. To obtain the probability of detection, 10^5 independent trials were run, and the test statistics are compared with the thresholds in order to obtain P_d. The probability of detection P_d is plotted as a function of the signal-to-noise-ratio, which is defined as $SNR = \gamma^{-1}\mathbf{s}^H\mathbf{s}$. The number of snapshots in the secondary data is set to $K = 20$.

We first consider a scenario in which $\theta = 0^\circ$, i.e., the actual and presumed steering vectors are perfectly aligned. The cone angle is chosen as $\theta_c = 12^\circ$. The probability of detection for the two detectors is shown in Fig. 2. Even in this situation where the ACE is expected to be very performant, the GLRT shows an improvement compared with the ACE; the difference is about 0.9 dB at $P_d = 0.8$. Note that this seemingly bewildering result does not contradict the theory of [14] as the GLRT is not invariant to G when $\mathbf{T}\bar{\mathbf{a}} \propto \bar{\mathbf{a}}$. Hence, the GLRT performs better than the ACE, certainly, but does not enjoy the natural invariances of the problem, which are given by (28)–(29) when $\theta = 0$. Nevertheless, it is an interesting feature that the GLRT does better than the ACE in the case of no mismatch.

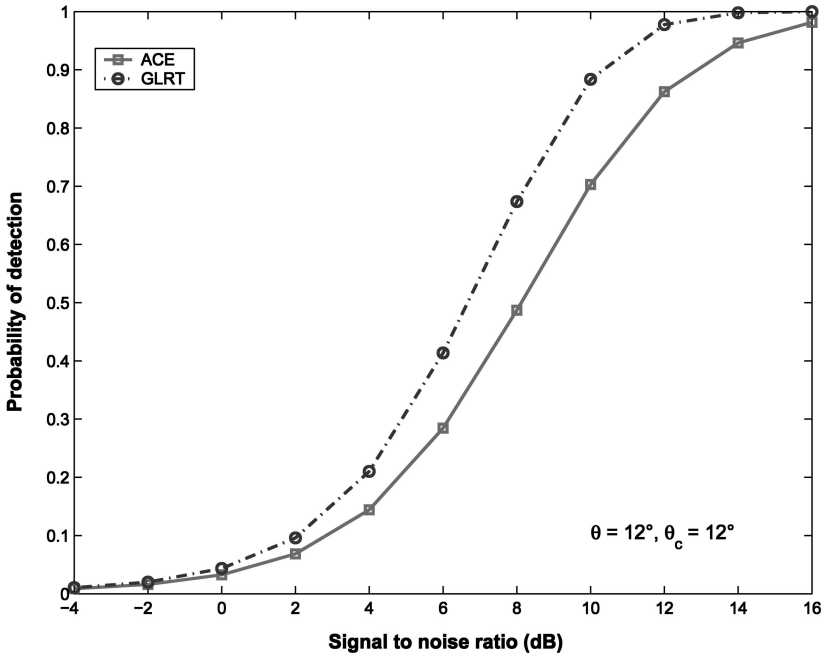

Fig. 3. Probability of detection versus SNR. $\theta = 12^\circ$ and $\theta_c = 12^\circ$.

Next, we assess the robustness of the detectors in the case of a mismatch between the actual and the presumed steering vectors. Towards this end, the actual steering vector is such that its angle with $\bar{\mathbf{a}}$ is $\theta = 12^\circ$. Similarly to the previous scenario, we have $\theta_c = 12^\circ$. The results are plotted in Fig. 3. From inspection of this figure, it can be seen that the GLRT outperforms the ACE; the difference at $P_d = 0.8$ is now about 2 dB. Therefore, in case of a steering vector mismatch, the GLRT offers an improved robustness compared with the ACE.

IV. CONCLUSIONS

We considered the problem of designing an adaptive detector that can take into account possible mismatches between the presumed steering vector and its actual value. Towards this end, we assumed that the steering vector of interest mostly belongs to a known linear subspace, but that a small fraction of its energy can lie outside this subspace. Using this modeling, we derived the GLRT and proposed a computationally efficient implementation of the MLE, using the theory of Lagrange multipliers. The proposed detector was shown to perform better than the ACE (at the price of an increased computational complexity), and offers additional robustness as it can accommodate deviations from the presumed steering vector. Further work should be devoted to robustness analysis of this detector under other types of mismatch. As a final remark, observe that increased robustness is usually traded for an increased sensitivity to unaccounted sidelobe targets. This issue is important and deserves further examination. A possible solution to mitigate this drawback is proposed in [31] where a detector decides whether a signal in the cone, or in its complement, is present.

APPENDIX A. PROBABILITY THAT $\mathbf{z}$ BELONGS TO THE CONE UNDER THE NULL HYPOTHESIS

In this appendix, we derive an expression for the probability that the test vector $\mathbf{z}$ lies inside the cone, when H_0 holds. For mathematical tractability, we assume that the covariance matrix of $\mathbf{z}$ is the identity matrix. Then, we have

$$\begin{aligned}\Pr(\mathbf{z} \in \mathcal{C} \mid H_0) &= \Pr\left(\frac{\mathbf{z}^H \mathbf{P}_{\bar{\mathbf{A}}} \mathbf{z}}{\mathbf{z}^H \mathbf{z}} \geq \rho\right) \\ &= \Pr\left(\frac{\mathbf{z}^H \mathbf{P}_{\bar{\mathbf{A}}} \mathbf{z}}{\mathbf{z}^H \mathbf{P}_{\bar{\mathbf{A}}}^{\perp} \mathbf{z}} \geq \frac{\rho}{1-\rho} = \zeta\right). \quad (35)\end{aligned}$$

However, under the assumption that $\mathbf{z} \sim \mathcal{N}(\mathbf{0}, \mathbf{I})$, $\mathbf{z}^H \mathbf{P}_{\bar{\mathbf{A}}} \mathbf{z}$ and $\mathbf{z}^H \mathbf{P}_{\bar{\mathbf{A}}}^{\perp} \mathbf{z}$ are independent random variables, distributed as χ_p^2 and χ_{m-p}^2. Therefore, $f = (\mathbf{z}^H \mathbf{P}_{\bar{\mathbf{A}}} \mathbf{z})/(\mathbf{z}^H \mathbf{P}_{\bar{\mathbf{A}}}^{\perp} \mathbf{z})$ has an F distribution and its pdf is given by

$$f_F(f) = \frac{\Gamma(m)}{\Gamma(p)\Gamma(m-p)} \frac{f^{p-1}}{(1+f)^m}. \quad (36)$$

Consequently,

$$\begin{aligned}\Pr(\mathbf{z} \in \mathcal{C} \mid H_0) &= \frac{\Gamma(m)}{\Gamma(p)\Gamma(m-p)} \int_{\zeta}^{\infty} \frac{f^{p-1}}{(1+f)^m} df \\ &= \frac{\Gamma(m)}{\Gamma(p)\Gamma(m-p)} \frac{\zeta^{p-m}}{m-p} \\ &\quad \times {}_2F_1\left(m, m-p; m-p+1; -\frac{1}{\zeta}\right) \quad (37)\end{aligned}$$

TABLE I
$\Pr(\mathbf{z} \in \mathcal{C} \mid H_0)$ Versus Cone Angle

θ_c	3°	6°	9°	12°	15°	18°
	1.157×10^{-18}	1.859×10^{-14}	5.256×10^{-12}	2.82×10^{-10}	6.053×10^{-9}	7.24×10^{-8}

Note: $m = 8$, $p = 1$, $\mathbf{z} \sim \mathcal{N}(\mathbf{0}, \mathbf{I})$.

where, to obtain the last expression, we made use of [32, eqn 3.194.2], with ${}_2F_1(-,-;-;-)$ denoting the hypergeometric function. Table I provides numerical values of this probability for different values of θ_c.

It can be observed that this probability is much smaller than the usual P_{fa} considered. However, it should be reminded that P_{fa} cannot be chosen lower than $\Pr(\mathbf{z} \in \mathcal{C} \mid H_0)$, which in turn implies that the cone angle θ_c should not be chosen too large.

OLIVIER BESSON
Dept. of Avionics and Systems
ENSICA
1 Place Emile Blouin
31056 Toulouse
France
E-mail: (besson@ensica.fr)

REFERENCES

[1] Gini, F., Farina, A., and Greco, M.
Selected list of references on radar signal processing.
IEEE Transactions on Aerospace and Electronic Systems, **37**, 1 (Jan. 2001), 329–359.

[2] Kelly, E. J.
An adaptive detection algorithm.
IEEE Transactions on Aerospace and Electronic Systems, **22**, 1 (Mar. 1986), 115–127.

[3] Robey, F. C., Fuhrmann, D. R., Kelly, E. J., and Nitzberg, R.
A CFAR adaptive matched filter detector.
IEEE Transactions on Aerospace and Electronic Systems, **28**, 1 (Jan. 1992), 208–216.

[4] Fabrizio, G. A., Farina, A., and Turley, M. D.
Spatial adaptive subspace detection in OTH radar.
IEEE Transactions on Aerospace and Electronic Systems, **39**, 4 (Oct. 2003), 1407–1428.

[5] De Maio, A., Foglia, G., Conte, E., and Farina, A.
CFAR behavior of adaptive detectors: An experimental analysis.
IEEE Transactions on Aerospace and Electronic Systems, **41**, 1 (Jan. 2005), 233–251.

[6] Scharf, L. L., and McWhorter, T.
Adaptive matched subspace detectors and adaptive coherence estimators.
In *Proceedings of the 30th Asilomar Conference on Signals and Systems Computers*, Pacific Grove, CA, Nov. 3–6 1996, 1114–1117.

[7] McWhorter, T., Scharf, L. L., and Griffiths, L. J.
Adaptive coherence estimation for radar signal processing.
In *Proceedings of the 30th Asilomar Conference on Signals and Systems Computers*, Pacific Grove, CA, Nov. 3–6 1996, 536–540.

[8] Scharf, L. L.
Statistical Signal Processing: Detection, Estimation and Time Series Analysis.
Reading, MA: Addison Wesley, 1991.

[9] Conte, E., Lops, M., and Ricci, G.
Asymptotically optimum radar detection in compound-Gaussian clutter.
IEEE Transactions on Aerospace and Electronic Systems, **31**, 2 (Apr. 1995), 617–625.

[10] Conte, E., Lops, M., and Ricci, G.
Adaptive matched filter detection in spherically invariant noise.
IEEE Signal Processing Letters, **3**, 8 (Aug. 1996), 248–250.

[11] Kraut, S., and Scharf, L. L.
The CFAR adaptive subspace detector is a scale-invariant GLRT.
IEEE Transactions on Signal Processing, **47**, 9 (Sept. 1999), 2538–2541.

[12] Conte, E., and De Maio, A.
An invariant framework for adaptive detection in partially homogeneous environment.
WSEAS Transactions on Circuits Systems, **2**, 1 (Jan. 2003), 282–287.

[13] Kraut, S., and Scharf, L. L.
UMP invariance of the multi-rank adaptive coherence estimator.
In *Proceedings of the 37th Asilomar Conference on Signals and Systems Computers*, Pacific Grove, CA, Nov. 9–12 2003, 1863–1867.

[14] Kraut, S., Scharf, L. L., and Butler, R. W.
The adaptive coherence estimator: A uniformly most powerful invariant adaptive detection statistic.
IEEE Transactions on Signal Processing, **53**, 2 (Feb. 2005), 427–438.

[15] Kelly, E. J.
Performance of an adaptive detection algorithm; rejection of unwanted signals.
IEEE Transactions on Aerospace and Electronic Systems, **25**, 2 (April 1989), 122–133.

[16] Kalson, S. Z.
An adaptive array detector with mismatched signal rejection.
IEEE Transactions on Aerospace and Electronic Systems, **28**, 1 (Jan. 1992), 195–207.

[17] Richmond, C. D.
Response of sample covariance based MVDR beamformer to imperfect look and inhomogeneities.
IEEE Signal Processing Letters, **2**, 12 (Dec. 1998), 325–327.

[18] Richmond, C. D.
Performance of a class of adaptive detection algorithms in nonhomogeneous environments.
IEEE Transactions on Signal Processing, **48**, 5 (May 2000), 1248–1262.

[19] Blum, R. S., and McDonald, K. F.
Analysis of STAP algorithms for cases with mismatched steering and clutter statistics.
IEEE Transactions on Signal Processing, **48**, 2 (Feb. 2000), 301–310.

[20] McDonald, K. F., and Blum, R. S.
Exact performance of STAP algorithms with mismatched steering and clutter statistics.
IEEE Transactions on Signal Processing, **48**, 10 (Oct. 2000), 2750–2763.

[21] Vorobyov, S. A., Gershman, A. B., and Luo, Z.
Robust adaptive beamforming using worst-case performance optimization: A solution to the signal mismatch problem.
IEEE Transactions on Signal Processing, **51**, 2 (Feb. 2003), 313–324.

[22] Li, J., Stoica, P., and Wang, Z.
On robust Capon beamforming and diagonal loading.
IEEE Transactions on Signal Processing, **51**, 7 (July 2003), 1702–1715.

[23] Li, J., Stoica, P., and Wang, Z.
Doubly constrained robust Capon beamformer.
IEEE Transactions on Signal Processing, **52**, 9 (Sept. 2004), 2407–2423.

[24] Lorenz, R., and Boyd, S. P.
Robust minimum variance beamforming.
IEEE Transactions on Signal Processing, **53**, 5 (May 2005), 1684–1696.

[25] Besson, O., Scharf, L. L., and Kraut, S.
Adaptive detection of a a signal known only to lie on a line in a known subspace, when primary and secondary data are partially homogeneous.
IEEE Transactions on Signal Processing, to be published.

[26] De Maio, A.
Robust adaptive radar detection in the presence of steering vector mismatches.
IEEE Transactions on Aerospace and Electronic Systems, **41**, 4 (Oct. 2005), 1322–1337.

[27] Ramprashad, S., Parks, T. W., and Shenoy, R.
Signal modeling and detection using cone classes.
IEEE Transactions on Signal Processing, **44**, 2 (Feb. 1996), 329–338.

[28] Boyd, S., and Vandenberghe, L.
Convex Optimization.
London: Cambridge University Press, 2004.

[29] Horn, R., and Johnson, C.
Matrix Analysis.
London: Cambridge University Press, 1990.

[30] Moon, T. K., and Stirling, W. C.
Mathematical Methods and Algorithms for Signal Processing.
Upper Saddle River, NJ: Prentice-Hall, 2000.

[31] Bandiera, F., De Maio, A., and Ricci, G.
Adaptive CFAR radar detection with conic rejection.
IEEE Transactions on Signal Processing, submitted for publication.

[32] Gradshteyn, I. S., and Ryzhik, I. M.
In A. Jeffrey (Ed.), *Table of Integrals, Series and Products* (5th ed.).
New York: Academic Press, 1994.

Multisensor Target Tracking Performance with Bias Compensation

In this paper, multisensor-multitarget tracking performance with bias estimation and compensation is investigated when only moving targets of opportunity are available. First, we discuss the tracking performance improvement with bias estimation and compensation for synchronous biased sensors, and then a novel bias estimation method is proposed for asynchronous sensors with time-varying biases. The performance analysis and simulations show that asynchronous sensors have a slightly degraded performance compared with the "equivalent" synchronous ones. The bias estimates as well as the corresponding Cramer-Rao lower bound (CRLB) on the covariance of the bias estimates, i.e., the quantification of the available information on the sensor biases in any scenario are also given. Tracking performance evaluations with different sources of biases—offset biases, scale biases, and sensor location uncertainties, are also presented and we show that tracking performance is significantly improved with bias estimation and compensation compared with the target tracking using the original biased measurements. The performance is also close to the lower bound obtained in the absence of biases.

I. INTRODUCTION

Registration error compensation is vital in multiple sensor systems in order to carry out data fusion. This requires estimation of the unknown sensor measurement biases. It is important to correct for these bias errors so that the multiple sensor measurements and/or tracks can be referenced as accurately as possible to a common tracking coordinate system (frame). If uncorrected, registration error can lead to large tracking errors and potentially to the formation of multiple tracks (ghosts) for the same target.

To estimate the bias vector, the classical approach is to augment the system state to include the bias vector as part of the state, then implement an augmented state Kalman filter (ASKF) by stacking the state of all the targets and the sensor biases into a single vector. The problem with this approach is that the implementation of this ASKF can be computationally infeasible. In addition, numerical

Manuscript received September 24, 2004; revised October 31, 2005; released for publication February 23, 2006.

IEEE Log No. T-AES/42/3/884477.

Refereeing of this contribution was handled by B. La Scala.